© 2015. Published by The Company of Biologists Ltd | Journal of Cell Science (2015) 128, 281–292 doi:10.1242/jcs.158337

RESEARCH ARTICLE

# Selective synaptic targeting of the excitatory and inhibitory presynaptic organizers FGF22 and FGF7

**Akiko Terauchi[1,2], Kendall M. Timmons[2], Koto Kikuma[2], Yvonne Pechmann[3], Matthias Kneussel[3] and Hisashi Umemori[1,2,4,*]**

## ABSTRACT

Specific formation of excitatory and inhibitory synapses is crucial for proper functioning of the brain. Fibroblast growth factor 22 (FGF22) and FGF7 are postsynaptic-cell-derived presynaptic organizers necessary for excitatory and inhibitory presynaptic differentiation, respectively, in the hippocampus. For the establishment of specific synaptic networks, these FGFs must localize to appropriate synaptic locations – FGF22 to excitatory and FGF7 to inhibitory postsynaptic sites. Here, we show that distinct motor and adaptor proteins contribute to intracellular microtubule transport of FGF22 and FGF7. Excitatory synaptic targeting of FGF22 requires the motor proteins KIF3A and KIF17 and the adaptor protein SAP102 (also known as DLG3). By contrast, inhibitory synaptic targeting of FGF7 requires the motor KIF5 and the adaptor gephyrin. Time-lapse imaging shows that FGF22 moves with SAP102, whereas FGF7 moves with gephyrin. These results reveal the basis of selective targeting of the excitatory and inhibitory presynaptic organizers that supports their different synaptogenic functions. Finally, we found that knockdown of SAP102 or PSD95 (also known as DLG4), which impairs the differentiation of excitatory synapses, alters FGF7 localization, suggesting that signals from excitatory synapses might regulate inhibitory synapse formation by controlling the distribution of the inhibitory presynaptic organizer.

**KEY WORDS: Fibroblast growth factor, Synapse specificity, Intracellular microtubule transport, Hippocampus, Excitatory/inhibitory balance**

## INTRODUCTION

Alterations in the balance of excitatory and inhibitory inputs to a neuron might lead to various neurological and psychiatric disorders, such as autism, schizophrenia and epilepsy (Möhler, 2006; Rubenstein and Merzenich, 2003; Singer and Minzer, 2003; Wassef et al., 2003). Thus, precise formation of excitatory and inhibitory synapses is crucial for proper brain function. Synapses form at sites where axons contact their target dendrites. Target-derived molecules play important roles in the differentiation of axons into functional presynaptic terminals (Fox and Umemori, 2006; Futai et al., 2013; Johnson-Venkatesh and Umemori, 2010; Missler et al., 2012; Siddiqui and Craig, 2011; Südhof, 2008). We have identified such presynaptic organizers by performing unbiased biochemical purification from developing mouse brains (Umemori et al., 2004; Umemori and Sanes, 2008). A group of molecules that we have identified belongs to the fibroblast growth factor (FGF) family, and we have shown that FGF22 and its close relatives FGF7 and FGF10 promote presynaptic differentiation in the cerebellum (Umemori et al., 2004) and at the neuromuscular junction (Fox et al., 2007). Remarkably, in the hippocampus, FGF22 and FGF7 have distinct roles – FGF22 selectively promotes excitatory presynaptic differentiation, whereas FGF7 promotes inhibitory presynaptic differentiation (Terauchi et al., 2010). The differentiation of excitatory or inhibitory nerve terminals on dendrites of CA3 pyramidal neurons is specifically impaired in mutants lacking FGF22 or FGF7, respectively, both *in vitro* and *in vivo*. Defects in excitatory and inhibitory presynaptic differentiation in FGF-knockout mice have a significant impact on brain function – FGF22-knockout mice are resistant to and FGF7-knockout mice are prone to epileptic seizures (Terauchi et al., 2010).

How do FGF22 and FGF7 accomplish their different effects on excitatory or inhibitory synapses? We have found previously that the different effects are mainly achieved by their distinct synaptic localizations – FGF22 localizes to excitatory and FGF7 to inhibitory postsynaptic sites (Terauchi et al., 2010). However, the molecular mechanisms by which these FGFs are selectively targeted to the specific type of synapses are unknown. A potential mechanism that operates fast and long-distance transport of molecules in neurons is intracellular transport by microtubule-dependent molecular motors such as the kinesin superfamily proteins (KIFs). The motor domain of KIFs binds to and moves along microtubules by ATP hydrolysis. The tail region of KIFs interacts with adaptor proteins, which recognize cargos containing specific molecules to be transported (Hirokawa et al., 2010; Hirokawa et al., 2009; Kardon and Vale, 2009; Millecamps and Julien, 2013). An appropriate combination of a motor protein and an adaptor protein appears to be important for accurate targeting of synaptic components (Dumoulin et al., 2009; Jeyifous et al., 2009; Setou et al., 2002; Terauchi and Umemori, 2012; Washbourne et al., 2004; Zheng et al., 2011). Here, we examine how the two presynaptic organizers FGF22 and FGF7 are transported to the appropriate locations so that they act as synapse-type-specific organizing molecules. We identify a combination of distinct motor and adaptor proteins that contributes to selective synaptic targeting of FGF22 and FGF7. Time-lapse imaging shows that scaffolding proteins at excitatory or inhibitory synapses serve as adaptor proteins for each FGF. Our results demonstrate novel molecular mechanisms that ensure accurate targeting of the

[1]Department of Neurology, F.M. Kirby Neurobiology Center, Boston Children's Hospital, Harvard Medical School, Boston, MA 02115, USA. [2]Molecular & Behavioral Neuroscience Institute, University of Michigan Medical School, Ann Arbor, MI 48109-2200, USA. [3]Center for Molecular Neurobiology, ZMNH, University Medical Center Hamburg-Eppendorf, Falkenried 94, D-20251 Hamburg, Germany. [4]Department of Biological Chemistry, University of Michigan Medical School, Ann Arbor, MI 48109-2200, USA.

*Author for correspondence (hisashi.umemori@childrens.harvard.edu)

**Received 17 June 2014; Accepted 20 November 2014**



Journal of Cell Science

Journal of Cell Science (2015) 128, 281–292 doi:10.1242/jcs.158337

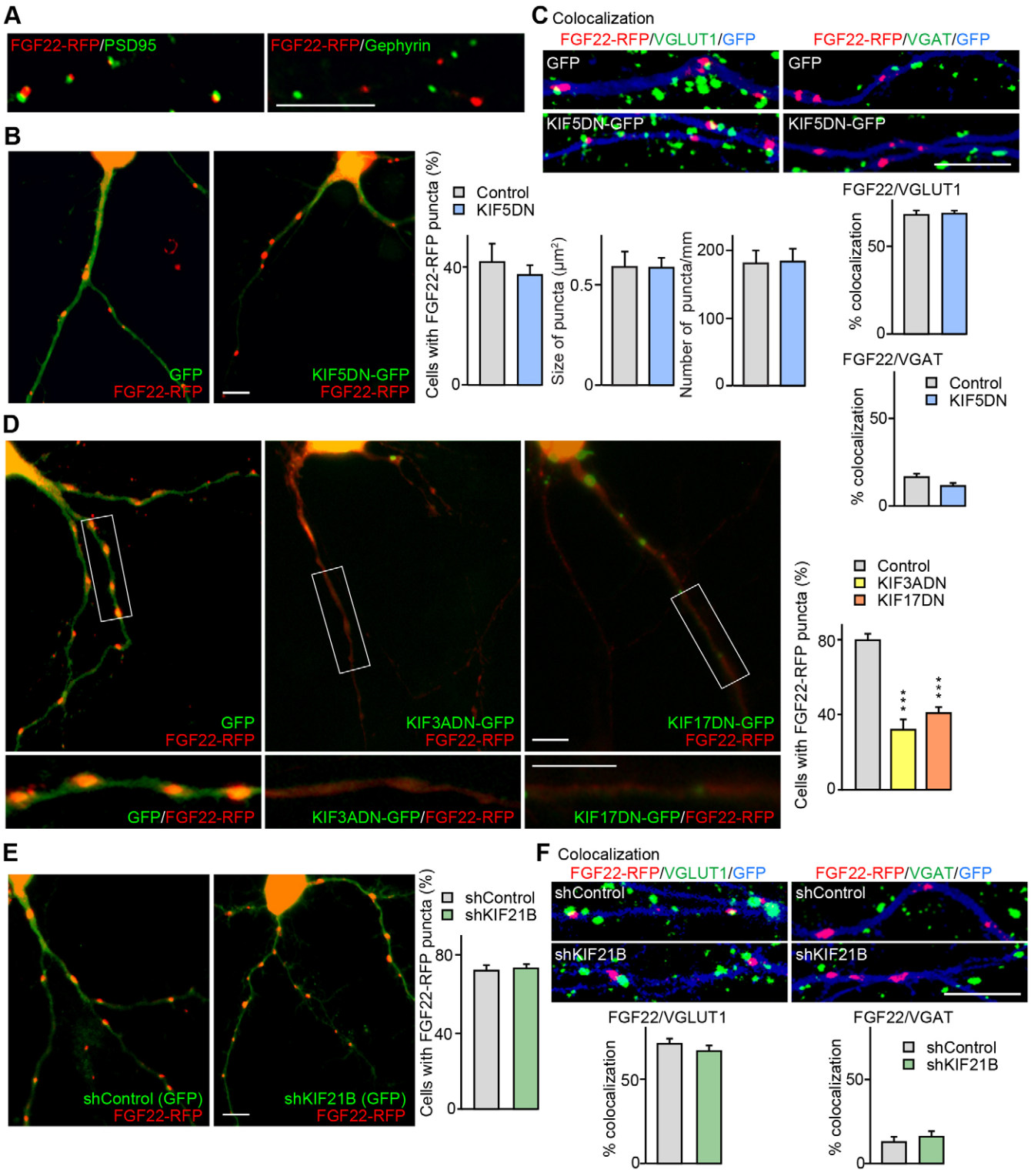


**Fig. 1.** See next page for legend.

synapse-type-specific presynaptic organizers for the precise formation of excitatory and inhibitory synapses and for proper functioning of the brain. Finally, we provide data suggesting that excitatory synapses might send signals to regulate the localization of FGF7 in order to control the balance between excitatory and inhibitory synapse formation.

## RESULTS

### Synaptic targeting of the excitatory presynaptic organizer FGF22 requires KIF3A and KIF17 function

The excitatory presynaptic organizer FGF22 localizes to excitatory synapses in the hippocampus for its function (Terauchi et al., 2010). To investigate the molecular

Journal of Cell Science (2015) 128, 281–292 doi:10.1242/jcs.158337

**Fig. 1. Molecular motors KIF3A and KIF17 are involved in the excitatory synaptic targeting of FGF22.** (A) FGF22–RFP localizes to excitatory synapses and not inhibitory synapses. Cultured hippocampal neurons were transfected with the plasmid encoding FGF22–RFP and stained with the anti-PSD95 or anti-gephyrin antibody. FGF22–RFP colocalizes with PSD95 but not with gephyrin. (B,C) Disruption of KIF5 function does not affect the percentage of cells with FGF22–RFP puncta, the size and density of FGF22–RFP puncta, or their targeting to excitatory synapses. Cultured hippocampal neurons were co-transfected with the plasmid encoding FGF22–RFP and the plasmid encoding GFP or KIF5DN–GFP at 7 DIV. Neurons were fixed and analyzed at 8 DIV. (B) Representative images of transfected neurons. Percentages of neurons with a punctate pattern of FGF22–RFP and the size and density of FGF22–RFP puncta are shown in the graphs to the right of the images. (C) Transfected neurons stained with the anti-VGLUT1 or anti-VGAT antibody. Percentages of FGF22 puncta colocalizing with VGLUT1 puncta or VGAT puncta are shown in the graphs below the images. (D) Disruption of the function of KIF3A or KIF17 decreases the percentage of cells with FGF22–RFP puncta. Cultured hippocampal neurons were co-transfected with the plasmids encoding FGF22–RFP and GFP (left), FGF22–RFP and KIF3ADN–GFP (middle) or FGF22–RFP and KIF17DN–GFP (right) at 6 DIV. Neurons were fixed and analyzed at 8 DIV. Higher-magnification views of the boxed areas are shown in the lower panels. The graph shows the percentages of neurons with a punctate pattern of FGF22–RFP. (E,F) shRNA-mediated knockdown of KIF21B does not alter the percentage of cells with FGF22–RFP puncta and their targeting to excitatory synapses. Cultured hippocampal neurons were co-transfected with the plasmids encoding FGF22–RFP and control shRNA or FGF22–RFP and KIF21B shRNA at 5 DIV. Neurons were fixed and analyzed at 8 DIV. (E) Representative images of transfected neurons. The percentages of neurons with a punctate pattern of FGF22–RFP are shown in the graph to the right of the images. (F) Transfected neurons stained with the anti-VGLUT1 or anti-VGAT antibody. Percentages of FGF22 puncta colocalizing with VGLUT1 puncta or VGAT puncta are shown in the graphs below the images. Data are from 7–10 coverslips (12 mm diameter; 113.04 $mm^2$) from at least five independent experiments (B,D,E, for analysis of the percentage of cells with FGF22–RFP puncta), from 14–19 fields (222.85×167.86 μm) from four to five independent experiments (for the size and density of FGF22–RFP puncta in B) and from 14–26 fields (159.89×159.89 μm) from at least three independent experiments (C,F). Quantitative data show the mean±s.e.m.; ***$P<0.001$ (versus control; ANOVA followed by Tukey test). Scale bars: 10 μm.

mechanisms underlying the excitatory synaptic targeting of FGF22, we generated a fluorescently tagged FGF22 protein, FGF22–RFP. When transfected into cultured hippocampal neurons, FGF22–RFP colocalized with PSD95 (also known as DLG4), a scaffolding protein at excitatory synapses, and not with gephyrin, a scaffolding protein at inhibitory synapses (Fig. 1A), indicating that FGF22–RFP is appropriately targeted to excitatory synapses. We first searched for molecular motors that are involved in the excitatory synaptic targeting of FGF22. We focused on four KIFs – KIF5, KIF3A, KIF17 and KIF21B, because these KIFs act as molecular motors for the intracellular transport of postsynaptic neurotransmitter receptors and/or are enriched in dendrites. KIF5 is involved in the transportation of the $GABA_A$ receptor, glycine receptor and AMPA receptor (Maas et al., 2006; Nakajima et al., 2012; Setou et al., 2002; Smith et al., 2006); KIF3A localizes to excitatory postsynaptic terminals and is involved in AMPA receptor transportation (Lin et al., 2012); KIF17 is a dendritic motor involved in NMDA receptor transportation (Jo et al., 1999; Setou et al., 2000); and KIF21B is highly enriched in dendrites (Marszalek et al., 1999). To examine whether these KIFs are involved in FGF22 transport, we generated GFP-tagged dominant negative (DN) mutants for KIF5, KIF3A and KIF17, and short hairpin RNA (shRNA) for KIF21B (Labonté et al., 2013). DN-KIFs, which are also known as 'headless' mutants, contain the cargo-binding domain and no motor domain (Chu et al., 2006; Falley et al., 2009; Sathish et al., 2009; Uchida et al., 2009), and are mainly restricted to the cell body. The advantage of the headless approach is that they still bind to cargos and prevent compensatory transport by alternative systems. We introduced these constructs into cultured hippocampal neurons together with FGF22–RFP and examined the distribution and excitatory synaptic targeting of FGF22–RFP in the dendrites. In the control neurons, FGF22–RFP showed a punctate pattern of distribution in dendrites (Fig. 1B) and colocalized with vesicular glutamate transporter 1 (VGLUT1), the marker of excitatory presynaptic terminals, but not with vesicular GABA transporter (VGAT), the marker of inhibitory presynaptic terminals (Fig. 1C), indicating that FGF22 preferentially localizes to excitatory synapses. The localization of FGF22–RFP as well as the size and density of FGF22–RFP puncta were maintained even when KIF5 function was disrupted by KIF5DN (Fig. 1B,C). However, in neurons in which KIF3A or KIF17 function was disrupted (KIF3ADN or KIF17DN), FGF22–RFP showed a diffuse pattern of distribution, and the percentage of cells with FGF22–RFP puncta was dramatically decreased (Fig. 1D). shRNA-mediated knockdown of KIF21B did not influence the pattern of FGF22–RFP distribution (Fig. 1E) or its excitatory synaptic localization (Fig. 1F). These results indicate that KIF3A and KIF17, and not KIF5 or KIF21B, are potential motors of FGF22 and contribute to the targeting of FGF22 to excitatory synapses.

### Synaptic targeting of the inhibitory presynaptic organizer FGF7 requires KIF5 function

The inhibitory presynaptic organizer FGF7 localizes to inhibitory synapses in the hippocampus for its function (Terauchi et al., 2010). The fluorescently tagged FGF7 protein FGF7–RFP was colocalized with gephyrin and not with PSD95 (Fig. 2A), confirming that FGF7–RFP is appropriately targeted to inhibitory synapses. To identify the molecular motors that contribute to the inhibitory synaptic targeting of FGF7, we examined the effect of KIF5DN, KIF3ADN, KIF17DN and shRNA for KIF21B on the distribution and synaptic localization of FGF7–RFP in cultured hippocampal neurons. Contrary to the case of FGF22, when KIF5 function was disrupted by KIF5DN, FGF7–RFP showed a diffuse pattern of distribution, and the percentage of cells with FGF7–RFP puncta was dramatically decreased relative to that of the control (Fig. 2B). Remaining FGF7–RFP puncta were no longer preferentially localized at VGAT-positive inhibitory synapses (Fig. 2B). By contrast, in neurons expressing KIF3ADN or KIF17DN, FGF7 still showed a punctate pattern, and there was no change in the percentage of cells with FGF7–RFP puncta compared to that of the control (Fig. 2C). Interestingly, however, KIF3ADN and KIF17DN expression affected the size of FGF7–RFP puncta and the localization of FGF7–RFP to inhibitory synapses, respectively (Fig. 2C,D). KIF21B knockdown did not affect the distribution and inhibitory synaptic localization of FGF7–RFP (Fig. 2E,F). These results indicate that KIF5 is a crucial motor protein for the transport of FGF7 to inhibitory synapses and that KIF3A and KIF17 affect (probably indirectly; see Discussion) the accumulation and localization of FGF7 at inhibitory synapses.

### FGF22 moves with SAP102, and FGF7 moves with gephyrin

Molecular motors recognize various cargos through distinct adaptor proteins (Hirokawa et al., 2010). We next searched for adaptor proteins involved in the transport of FGF22 and FGF7.

Journal of Cell Science (2015) 128, 281–292 doi:10.1242/jcs.158337

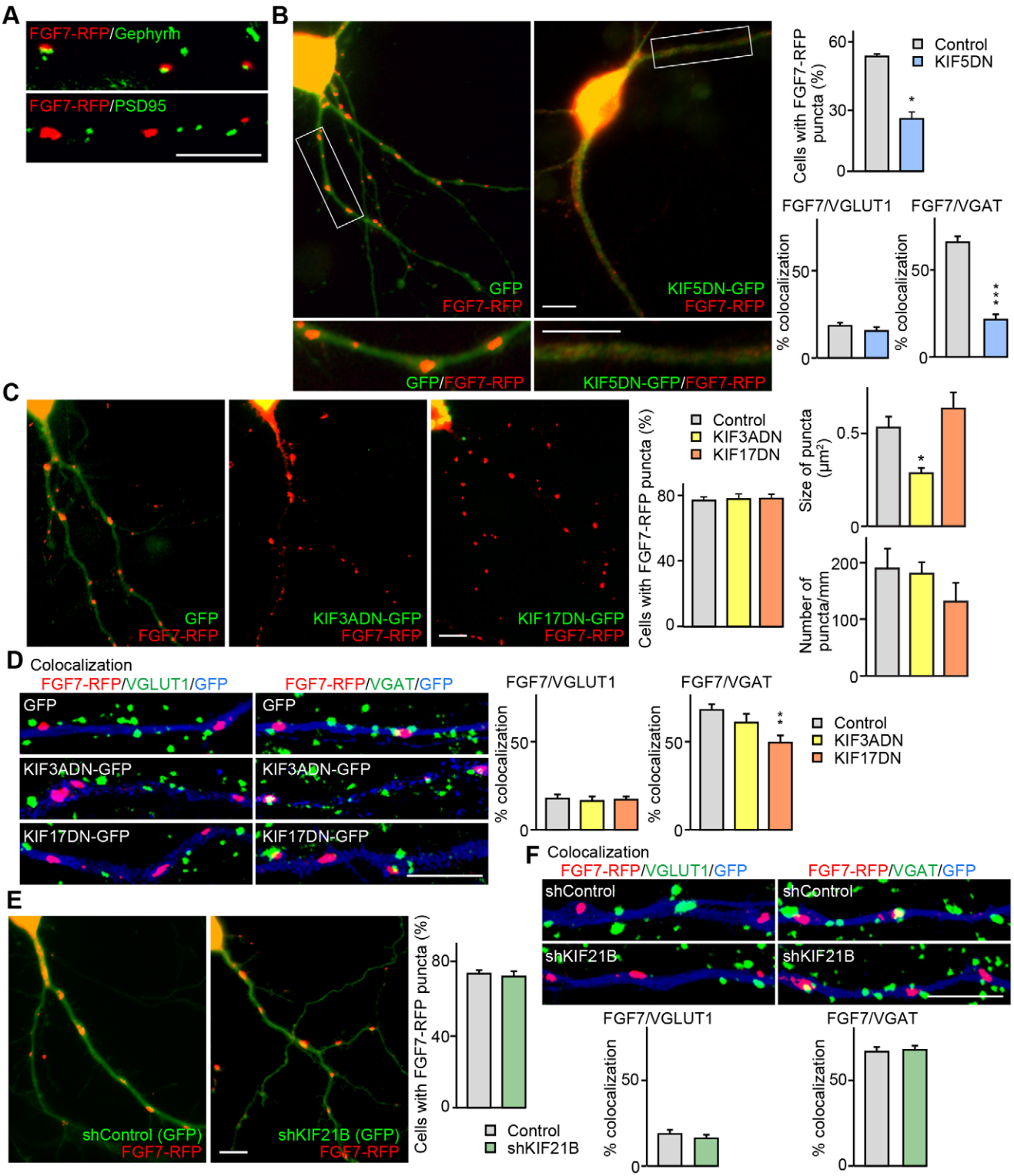


**Fig. 2.** See next page for legend.

Postsynaptic scaffolding proteins often serve as adaptor proteins for synaptic transportation of neurotransmitter receptors (Kneussel, 2005). We thus focused on scaffolding proteins at excitatory and inhibitory synapses – PSD95, SAP102 (also known as DLG3) and gephyrin, which in fact act as adaptor proteins for glutamate receptors (PSD95 and SAP102), $GABA_A$ and glycine receptors (gephyrin) (Chen et al., 2012; Dumoulin et al., 2009; Lau and Zukin, 2007; Maas et al., 2006; Zheng et al., 2011). To examine whether these scaffolding proteins act as adaptor proteins for FGF22 and FGF7, we performed live-imaging experiments with fluorescent-protein-tagged FGFs and scaffolding proteins. Because SAP102 and gephyrin bind to distinct motor proteins

**Fig. 2. Molecular motor KIF5 is essential for inhibitory synaptic targeting of FGF7.** (A) FGF7–RFP localizes to inhibitory synapses and not excitatory synapses. Cultured hippocampal neurons were transfected with the plasmid encoding FGF7–RFP and stained for gephyrin or PSD95. FGF7–RFP colocalizes with gephyrin but not with PSD95. (B) Disruption of KIF5 function decreases the percentage of cells with FGF7–RFP puncta and their localization to inhibitory synapses. Cultured hippocampal neurons were co-transfected with plasmids encoding FGF7–RFP and GFP (left) or FGF7–RFP and KIF5DN–GFP (right) at 7 DIV. Neurons were fixed, stained and analyzed at 8 DIV. Higher-magnification views of the boxed areas are shown in the lower panels. The upper graph shows the percentages of neurons with a punctate pattern of FGF7–RFP. The lower graphs show the percentages of FGF7 puncta colocalizing with VGLUT1 puncta or VGAT puncta. (C,D) Cultured hippocampal neurons were co-transfected with plasmids encoding FGF7–RFP and GFP, FGF7–RFP and KIF3ADN–GFP or FGF7–RFP and KIF17DN–GFP at 6 DIV. Neurons were fixed, stained and analyzed at 8 DIV. (C) Disruption of the function of KIF3A or KIF17 does not affect the percentage of cells with FGF7–RFP puncta, but the FGF7–RFP puncta in KIF3ADN-expressing cells are smaller than those in control neurons. Percentages of neurons with a punctate pattern of FGF7–RFP and the size and density of FGF7–RFP puncta are shown in the graphs to the right of the images. (D) Transfected cells were stained for VGLUT1 or VGAT. Percentages of FGF7 puncta colocalizing with VGLUT1 puncta or VGAT puncta are shown in the graphs to the right of the images. KIF17DN expression decreased the inhibitory synaptic targeting of FGF7. (E,F) shRNA-mediated knockdown of KIF21B does not alter the percentage of cells with FGF7–RFP puncta and the targeting of FGF7 to inhibitory synapses. Cultured hippocampal neurons were co-transfected with the plasmids encoding FGF7–RFP and control shRNA or FGF7–RFP and KIF21B shRNA at 5 DIV. Neurons were fixed, stained and analyzed at 8 DIV. (E) Representative images of transfected neurons. The graph shows the percentages of neurons with a punctate pattern of FGF7–RFP. (F) Transfected neurons stained for VGLUT1 or VGAT. Percentages of FGF7 puncta colocalizing with VGLUT1 puncta or VGAT puncta are shown in the graphs below the images. Data are from 6–9 coverslips (12 mm diameter; 113.04 $mm^2$) from at least five independent experiments (B,C,E, for analysis of the percentage of cells with FGF7–RFP puncta), from 14–22 fields (159.89×159.89 μm) from at least three independent experiments (for percentage colocalization in B,D,F) or from 10–13 fields (222.85×167.86 μm) from at least three independent experiments (C, for the size and density of FGF7–RFP puncta). All quantitative data show the mean±s.e.m.; *$P<0.05$; **$P<0.01$; ***$P<0.001$ [versus control; Student's *t*-test (B) or ANOVA followed by Tukey test (C,D)]. Scale bars: 10 μm.

and do not traffic together (Dumoulin et al., 2009; Elias et al., 2008; Lau and Zukin, 2007; Murata and Constantine-Paton, 2013; Nakajima et al., 2012; Sans et al., 2003; Tyagarajan and Fritschy, 2014), we used co-transportation of these two proteins as a control. As shown in Fig. 3A,B, 22.39±4.8% (mean±s.e.m.) of moving SAP102 was moving with gephyrin, and 21.91±4.3% of moving gephyrin was moving with SAP102. Thus, in our experiments, ~22% of co-transportation is considered as background. When neurons were co-transfected with SAP102 and FGF7, 30.58±5.7% of SAP102 puncta were moving together with FGF7 puncta (Fig. 3A; not significantly different from SAP102–gephyrin co-transportation). Similarly, 20.95±6.3% of gephyrin puncta were moving with FGF22 puncta (Fig. 3B; not significantly different from gephyrin–SAP102 co-transportation). By contrast, when hippocampal neurons were co-transfected with SAP102 and FGF22, we found that 73.34±4.7% of SAP102 puncta were moving together with FGF22 (Fig. 3A; $P<0.001$ compared to SAP102–gephyrin co-transportation), and 52.99±5.0% of FGF22 puncta were moving together with SAP102 puncta (Fig. 3C; $P<0.001$ compared to FGF22-gephyrin co-transportation). When hippocampal neurons were co-transfected with gephyrin and FGF7, 70.09±6.9% of gephyrin puncta were moving with FGF7 puncta (Fig. 3B; $P<0.001$ compared to gephyrin–SAP102 co-transportation), and 50.85±4.2% of FGF7 puncta were moving together with gephyrin puncta (Fig. 3D; $P<0.001$ compared to FGF7–SAP102 co-transportation). These results indicate that FGF22 preferentially moves with SAP102 and that FGF7 preferentially moves with gephyrin (Fig. 3E,F), suggesting that SAP102 and gephyrin serve as adaptor proteins for the transportation of FGF22 and FGF7, respectively. The average velocities of FGF22 and FGF7 puncta were 0.52±0.058 μm/s and 0.52±0.069 μm/s, respectively, which are consistent with KIF-dependent microtubule transport in dendrites (~0.3–0.8 μm/s; Adachi et al., 2005; Guillaud et al., 2003; Nakajima et al., 2012).

To exclude the possibility that FGFs are transported along the plasma membrane, we tested whether these FGFs can be detected by immunostaining in the absence of detergent permeabilization. For this, we have transfected plasmid encoding FGF22–GFP or FGF7–GFP together with the mCherry plasmid (to identify transfected neurons) into cultured hippocampal neurons and stained them in the presence or absence of detergent; FGF22–GFP or FGF7–GFP was visualized by staining the neurons with the anti-GFP antibody followed by the Alexa-Fluor-647-conjugated secondary antibody, and not by the GFP fluorescence. FGF22 and FGF7 staining was only detected in the presence of detergent (supplementary material Fig. S1), suggesting that FGFs are indeed transported by intracellular transport, rather than along the plasma membrane.

## SAP102 is crucial for the excitatory synaptic targeting of FGF22

Live-imaging analysis showed that FGF22, which localizes to excitatory synapses (Fig. 1A,C,F; Terauchi et al., 2010), preferentially moves with SAP102. We next examined whether SAP102 is necessary for the synaptic targeting of FGF22. For this, we silenced SAP102, PSD95 and gephyrin using shRNA, and analyzed the distribution and excitatory synaptic targeting of FGF22 in cultured neurons. shRNA constructs that we generated effectively reduced the amount of corresponding scaffolding proteins in hippocampal neurons as assessed by immunostaining (Fig. 4A). FGF22–GFP showed a punctate pattern of distribution in control shRNA-transfected neurons (Fig. 4B,C). This pattern was maintained in gephyrin-knockdown neurons and PSD95-knockdown neurons (Fig. 4B,C). The size, number and intensity of FGF22–GFP puncta in gephyrin- and PSD95-knockdown neurons were virtually the same as those in control neurons (Fig. 4D). In addition, FGF22–GFP still preferentially localized to glutamatergic and not GABAergic synapses in gephyrin- and PSD95-knockdown neurons (Fig. 4E). Thus, gephyrin and PSD95 are not necessary for the targeting of FGF22 to excitatory synapses. By contrast, in SAP102-knockdown neurons, FGF22–GFP showed a diffuse pattern of distribution, and the percentage of cells with FGF22–GFP puncta was dramatically decreased relative to that of the control (Fig. 4B,C). These results suggest that SAP102 plays crucial roles in the synaptic targeting of FGF22.

## Gephyrin is crucial for the inhibitory synaptic targeting of FGF7

Live-imaging analysis showed that FGF7, which localizes to inhibitory synapses (Fig. 2A,B,D,F; Terauchi et al., 2010), preferentially moves with gephyrin. To address whether gephyrin is necessary for the synaptic targeting of FGF7, we analyzed FGF7 distribution in the absence of gephyrin. In control

Journal of Cell Science (2015) 128, 281–292 doi:10.1242/jcs.158337

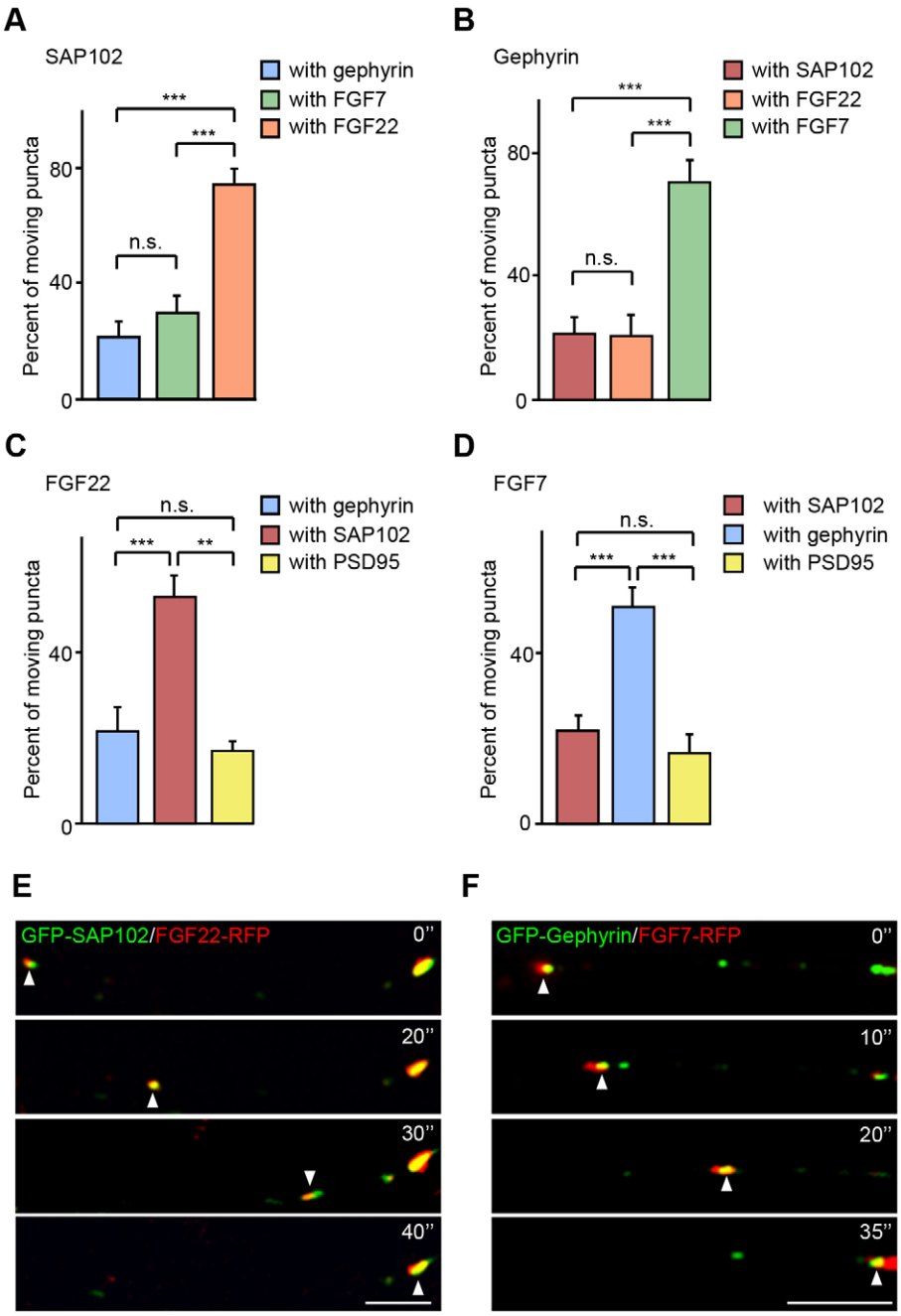


**Fig. 3. FGF22 moves with SAP102, whereas FGF7 moves with gephyrin.** (A–F) Cultured hippocampal neurons were transfected with expression plasmids at 1–3 DIV and observed at 5–7 DIV by live imaging. (A) Quantification of the percentage of co-transportation, focusing on GFP–SAP102-positive moving puncta. The interaction of GFP–SAP102 with RFP–gephyrin serves as control. The percentage of GFP–SAP102 moving with FGF7–RFP is similar to that moving with RFP–gephyrin. By contrast, a significantly higher percentage of GFP–SAP102 moves with FGF22–RFP than with RFP–gephyrin or FGF7–RFP. (B) Quantification of the percentage of co-transportation, focusing on GFP–gephyrin-positive moving puncta. Interaction of GFP–gephyrin with RFP–SAP102 serves as control. The percentage of GFP–gephyrin moving with FGF22–RFP is similar to that moving with RFP–SAP102. By contrast, a significantly higher percentage of GFP–gephyrin moves with FGF7–RFP than with RFP–SAP102 or FGF22–RFP. (C) Quantification of the percentage of co-transportation, focusing on FGF22–RFP-positive moving puncta. Compared to the interaction of FGF22–RFP with GFP–gephyrin, a significantly higher percentage of FGF22–RFP moves with GFP–SAP102. The percentage of FGF22–RFP moving with PSD95–GFP is similar to that moving with GFP–gephyrin. (D) Quantification of the percentage of co-transportation, focusing on FGF7–RFP-positive moving puncta. Compared to the interaction of FGF7–RFP with GFP–SAP102, a significantly higher percentage of FGF7–RFP moves with GFP–gephyrin. The percentage of FGF7–RFP moving with PSD95–GFP is similar to that moving with GFP–SAP102. Data are from 5–20 dendrites from at least three independent experiments (A,C) or from 10–17 dendrites from at least three independent experiments (B,D). All quantitative data show the mean±s.e.m.; $^{**}P<0.01$; $^{***}P<0.001$; n.s., not significant (ANOVA followed by Tukey test). (E,F) Representative time-lapse images of FGF22–RFP and GFP–SAP102 (E) and FGF7–RFP and GFP–gephyrin (F). Arrowheads indicate a co-transported punctum. Scale bars: 5 μm.

shRNA-transfected neurons, FGF7–GFP showed a punctate pattern of distribution (Fig. 5A,B), localizing at inhibitory synapses (Fig. 5D). However, when gephyrin was knocked down, FGF7–GFP showed a diffuse pattern of distribution, and the percentage of neurons with FGF7–GFP puncta was markedly decreased (Fig. 5A,B). These results indicate that gephyrin plays a crucial role in FGF7 targeting.

### Knockdown of SAP102 or PSD95 affects the localization of FGF7 to inhibitory synapses

When SAP102 or PSD95 was knocked down, there was no significant effect on the percentage of neurons with FGF7–GFP puncta (Fig. 5A,B), which is consistent with our live-imaging results that FGF7 does not preferentially move with SAP102 or PSD95 (Fig. 3D). However, we noticed that SAP102 knockdown significantly increased the size of FGF7–GFP puncta relative to that of the control, without changing their density (Fig. 5C). Those large FGF7–GFP puncta were mostly localized in the main dendrite and not in the branch (supplementary material Fig. S2). We hence examined the possibility that the synaptic localization of FGF7 might be altered in SAP102-knockdown neurons. In control shRNA-transfected neurons, FGF7–GFP localized to inhibitory and not excitatory synapses (Fig. 5D). By contrast, significantly less FGF7–GFP localized to inhibitory synapses in SAP102-knockdown neurons (Fig. 5D). Interestingly, a similar decrease in the inhibitory synaptic localization of FGF7–GFP was also found in PSD95-knockdown neurons (Fig. 5D). There was no increase in the excitatory synaptic localization of FGF7–GFP in SAP102- and PSD95-knockdown neurons (Fig. 5D). These results indicate that in the absence of SAP102 or PSD95, FGF7

Journal of Cell Science (2015) 128, 281–292 doi:10.1242/jcs.158337

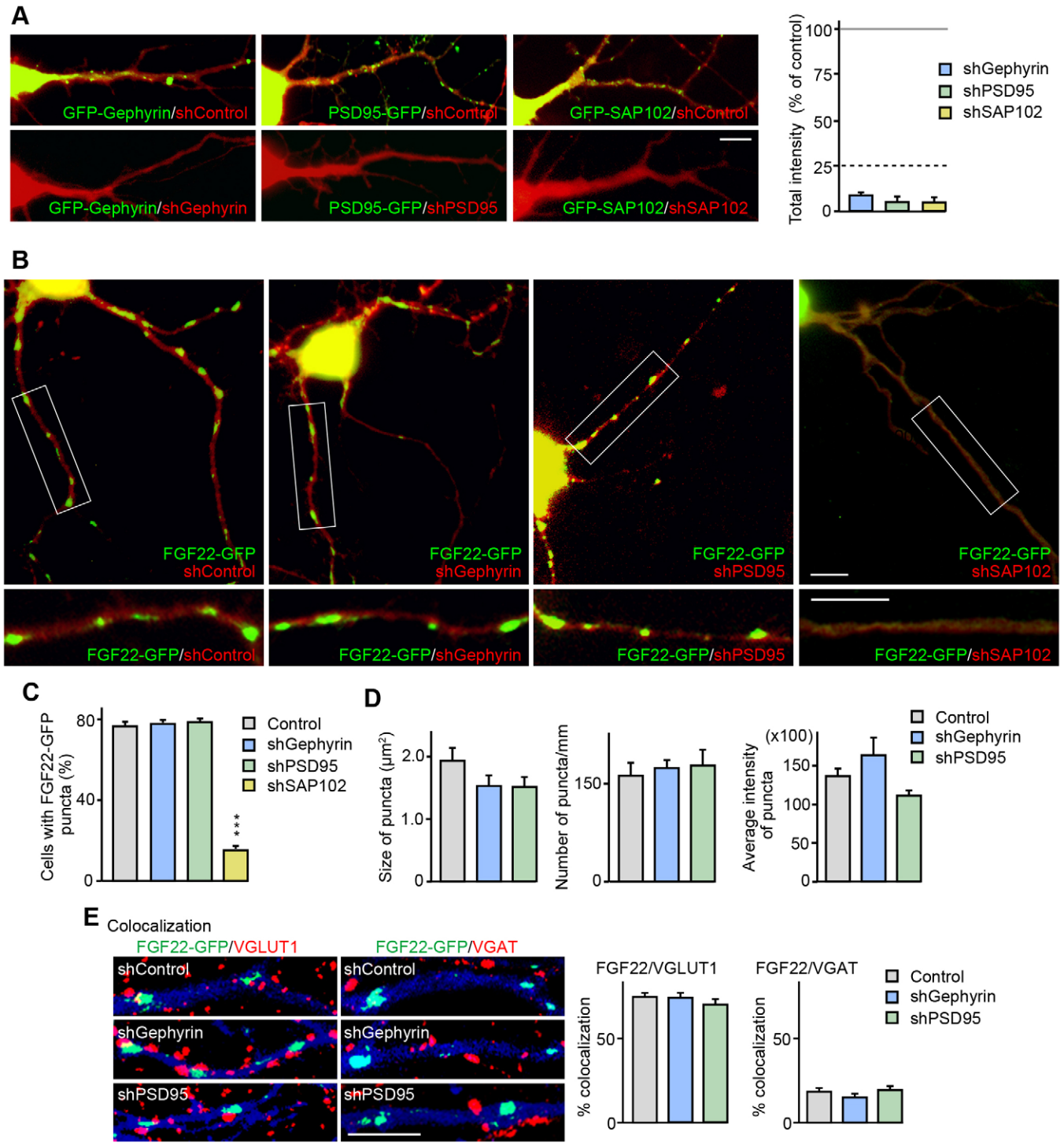


**Fig. 4.** See next page for legend.

localizes to non-synaptic domains rather than inhibitory synapses. This alteration might be an indirect effect of SAP102 or PSD95 knockdown, because SAP102 or PSD95 does not appear to be an adaptor for FGF7 transport (Fig. 3A,D). Given that SAP102 and PSD95 have clear roles in excitatory synaptic differentiation (Ehrlich et al., 2007; Elias et al., 2008; Elias and Nicoll, 2007; Murata and Constantine-Paton, 2013; Zheng et al., 2011), the change in the FGF7 localization in SAP102- and PSD95-knockdown neurons might be a consequence of impaired excitatory synaptic differentiation (see Discussion).

## DISCUSSION

Synaptic organizers such as FGFs, neuroligins, Ephs/ephrins, WNTs, SynCAMs, netrin-G ligands (NGLs), leucine-rich repeat transmembrane proteins (LRRTMs) and signal regulatory proteins (SIRPs) play crucial roles in the organization of synaptic connections

Journal of Cell Science (2015) 128, 281–292 doi:10.1242/jcs.158337

**Fig. 4. SAP102 is required for the targeting of FGF22 to excitatory synapses.** (A) Silencing of gephyrin, PSD95 and SAP102 by shRNA. Lower panels, cultured hippocampal neurons were transfected with plasmids encoding GFP–gephyrin and gephyrin shRNA (left), PSD95–GFP and PSD95 shRNA (middle) or GFP–SAP102 and SAP102 shRNA (right) at 3 DIV. Upper panels, control cultures were transfected with the plasmids encoding control shRNA and each fluorescently tagged scaffolding protein. Neurons were fixed at 5 DIV. The total GFP intensity in the transfected cells (shown as a percentage of the intensity in controls) was analyzed and is shown in the graph. All three shRNAs effectively inhibited the expression of corresponding scaffolding proteins (to <25% of their expression in controls). (B–E) Cultured hippocampal neurons were transfected with the plasmid encoding FGF22–GFP together with the plasmid encoding either control shRNA, gephyrin shRNA, PSD95 shRNA or SAP102 shRNA at 3 DIV. Neurons were fixed, stained and analyzed at 7 DIV. (B) Representative images of FGF22–GFP distributions in shRNA-transfected neurons. Higher-magnification views of the boxed areas are shown in the lower panels. (C) Percentages of neurons with a punctate pattern of FGF22–GFP. SAP102 knockdown decreases the percentage of neurons with FGF22–RFP puncta. (D) Quantification of the size, density and intensity of FGF22–GFP puncta in control, gephyrin-knockdown and PSD95-knockdown neurons. Gephyrin or PSD95 knockdown does not significantly affect the size, density or intensity of FGF22–GFP puncta. (E) Transfected neurons were stained for VGLUT1 or VGAT. Percentages of FGF22 puncta colocalizing with VGLUT1 puncta or VGAT puncta are shown in the graphs to the right of the images. Silencing gephyrin or PSD95 does not alter the targeting of FGF22 to excitatory synapses. Data are from 9–12 coverslips (12 mm diameter; 113.04 $mm^2$) from at least three independent experiments (C) or 14–16 fields (113.04 $mm^2$ for D; 159.89×159.89 μm for E) from at least four independent experiments (D,E). All quantitative data show the mean±s.e.m.; ***$P<0.001$ (versus control; ANOVA followed by Tukey test). Scale bars: 10 μm.

during development (Dalva et al., 2007; Fox and Umemori, 2006; Johnson-Venkatesh and Umemori, 2010; Linhoff et al., 2009; Umemori and Sanes, 2008; Waites et al., 2005). For the establishment of specific synaptic networks in the brain, synapse-type-specific organizers must localize to appropriate synaptic locations for their function. Here, we identified the molecular mechanisms underlying the transportation of the excitatory and inhibitory presynaptic organizers FGF22 and FGF7 to their appropriate synaptic sites. We found that the transport complexes for FGF22 and FGF7 consisted of distinct molecular motor and adaptor proteins. Our results reveal the basis of selective targeting of excitatory or inhibitory synapse-specific synaptic organizers that supports their different synaptogenic functions. This also implies that, depending on their function, two molecules in the same family can be transported to distinct locations by a specific combination of motor proteins and adaptor proteins.

For the excitatory presynaptic organizer FGF22, we found that motor proteins KIF3A and KIF17 and a scaffolding protein at excitatory synapses, SAP102, contribute to the targeting of the protein to excitatory synapses. Accumulating data suggest that KIF3A, KIF17 and SAP102 are involved in the early stage of excitatory synapse formation: (1) KIF3A appears to transport the GluR2 subunit to newly formed dendritic processes after light-induced retinal degeneration (Lin et al., 2012); (2) KIF17 transports NMDA receptors containing the GluN2B subunit (Setou et al., 2000), which is the dominant GluN2 subunit in the early stage of synaptic development (Bellone and Nicoll, 2007); and (3) SAP102 is expressed earlier than PSD95 (Elias et al., 2008; Sans et al., 2000) and has a role in trafficking and anchoring of the GluN2B subunit to immature synapses (Washbourne et al., 2004). As synaptogenesis proceeds, SAP102-dependent functions are shifted to PSD95-dependent functions, including an increase in the number of synaptic AMPA receptors and a switch of the NMDA receptor subunit from GluN2B to GluN2A (Elias et al., 2008; Sanz-Clemente et al., 2013). The use of KIF3A, KIF17 and SAP102, and not PSD95, for FGF22 targeting is consistent with the function of FGF22 during the early stage of synaptogenesis; both *in vitro* and *in vivo*, FGF22 is important for the initial formation of excitatory synapses in the hippocampus (Terauchi et al., 2010; Toth et al., 2013). The dependence of FGF22 targeting on SAP102 might contribute to the temporal specificity of FGF22 function. Note that in our experiments, ∼30% of cells expressing KIF3ADN or KIF17DN still had FGF22 puncta, which could be due to imperfect suppression of KIFs or functional redundancy among KIF proteins. In the experiments described in Fig. 1D, KIFDNs were expressed for just 2 days, as longer expression of KIFDNs eventually affected the viability of the cells. Thus, it is possible that the suppression by KIFDNs was not perfect. Also, as both KIF3A and KIF17 contribute to FGF22 transportation, these KIFs might have redundant functions. In addition, our results show that 52.99±5.01%, and not 100%, of FGF22 moves with SAP102 (Fig. 3C). This might be because there are additional adaptor proteins for FGF22.

In the case of the inhibitory presynaptic organizer FGF7, we found that the motor protein KIF5 and gephyrin, a scaffolding protein at inhibitory synapses, have crucial roles in transport to inhibitory synapses. KIF5 conveys many synaptic cargos (Hirokawa et al., 2009), including those targeted to inhibitory synapses as well as excitatory synapses. KIF5 transports $GABA_A$ receptors in cortical neurons by binding to Huntingtin-associated protein 1 (HAP1) (Twelvetrees et al., 2010) and in hippocampal neurons by binding to $GABA_A$R-associated protein complexes (Nakajima et al., 2012). KIF5 also transports glycine receptors by binding to gephyrin (Maas et al., 2009; Maas et al., 2006). At the same time, KIF5 transports the AMPA receptor subunit GluA2 with HAP1 towards excitatory synapses (Mandal et al., 2011). Therefore, for the inhibitory synaptic targeting of FGF7, gephyrin seems to be the essential component of the transport complex that gives specificity to travel to the inhibitory synapse.

KIFs are microtubule-dependent molecular motors that convey various synaptic cargos (Hirokawa and Noda, 2008; Hirokawa et al., 2009). KIF-mediated transport of membrane or secreted molecules in dendrites is relatively rapid, ranging from 0.3 μm/s to 0.8 μm/s. For example, the velocity of KIF17 during GluN2B transport is 0.76 μm/s (Guillaud et al., 2003) and that of KIF5A is 0.33 μm/s during the transport of $GABA_A$ receptors (Nakajima et al., 2012). Brain-derived neurotropic factor (BDNF) is transported at 0.47 μm/s (Adachi et al., 2005). Our live-imaging experiments also showed rapidly moving transport puncta of FGF22–RFP and FGF7–RFP; the average velocity was 0.52±0.058 μm/s for FGF22–RFP and 0.52±0.069 μm/s for FGF7–RFP. These velocities are consistent with the speed of KIF-dependent transport in dendrites, supporting the notion that microtubule-based transport operates the intracellular delivery of FGF22 and FGF7. Once these FGFs are transported to the synaptic regions, where actin filaments are the major cytoskeletal structure, actin-based transport by myosins might take over for the final delivery of FGFs to the surface of postsynaptic terminals (Hirokawa et al., 2010; Kneussel and Wagner, 2013).

An interesting question is how FGF22- and FGF7-harboring secretory vesicles are recognized by their specific adaptors. Given that FGF22 and FGF7 differ in their N-terminal sequence, it is possible that the N-terminal domains contain the signal for

Journal of Cell Science (2015) 128, 281–292 doi:10.1242/jcs.158337

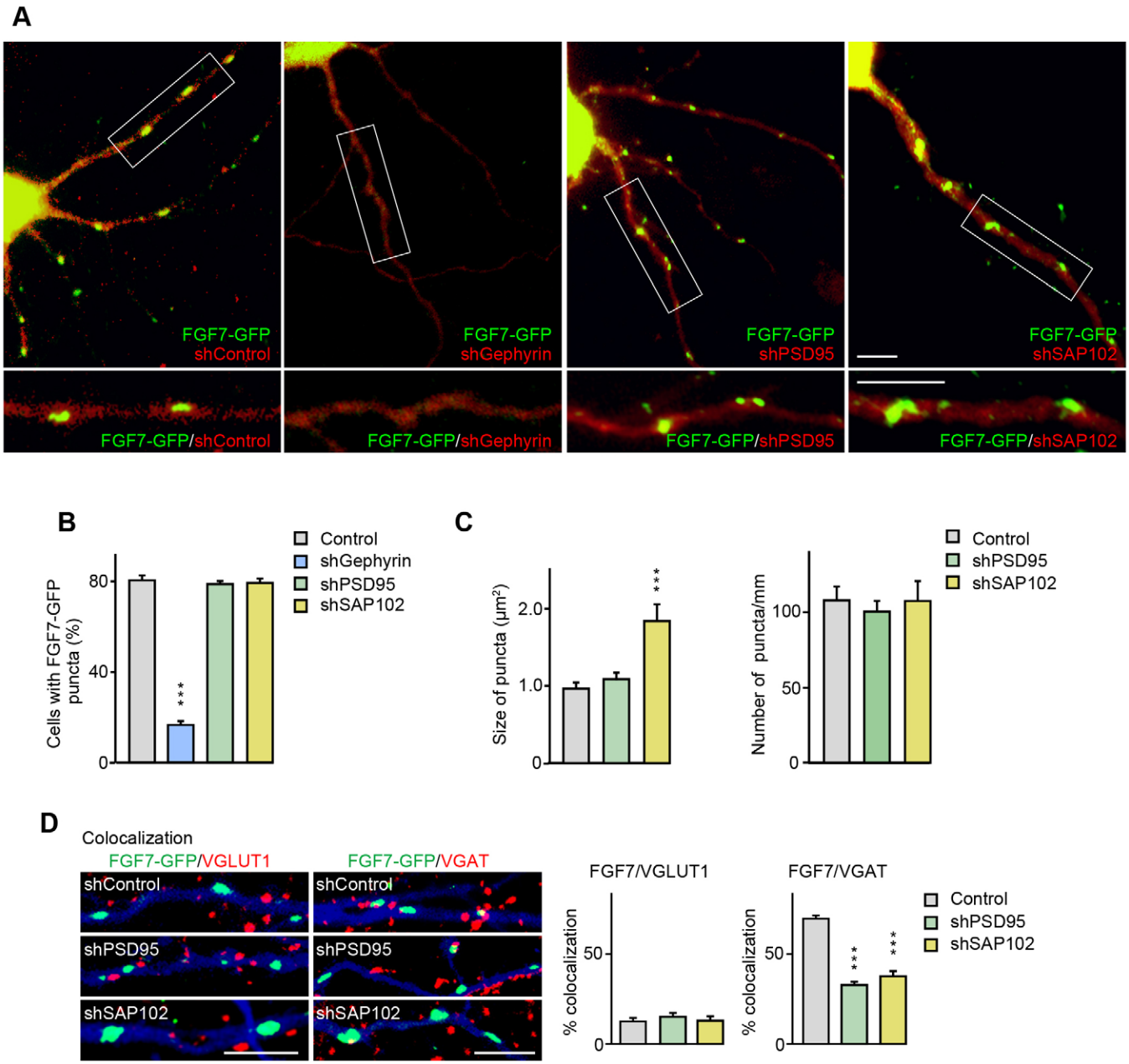


**Fig. 5. Gephyrin is required for inhibitory synaptic targeting of FGF7, and SAP102 and PSD95 knockdown influences FGF7 localization to inhibitory synapses.** Cultured hippocampal neurons were co-transfected with plasmid encoding FGF7–GFP and plasmid encoding control shRNA, gephyrin shRNA, PSD95 shRNA or SAP102 shRNA at 3 DIV. Neurons were fixed, stained and analyzed at 7 DIV. (A) Representative images of FGF7–GFP distributions in shRNA-transfected neurons. Higher-magnification views of the boxed areas are shown in the lower panels. (B) Percentages of neurons showing a punctate pattern of FGF7–GFP. Gephyrin knockdown decreases the percentage of cells with FGF7–GFP puncta. (C) Quantification of the size and density of FGF7–GFP puncta in control, PSD95-knockdown and SAP102-knockdown neurons. In SAP102-knockdown neurons, FGF7–GFP puncta were larger in size than in control neurons, with no change in the puncta density. (D) Transfected neurons were stained for VGLUT1 or VGAT. Percentages of FGF7 puncta colocalizing with VGLUT1 puncta or VGAT puncta are shown in the graphs. Silencing PSD95 or SAP102 decreased FGF7 localization to inhibitory synapses without increasing its localization to excitatory synapses. Data are from 13–17 coverslips (12 mm diameter; 113.04 $mm^2$) from at least five independent experiments (A–C) or 18–29 fields (159.89×159.89 μm) from at least four independent experiments (D). All quantitative data show the mean±s.e.m.; ***$P<0.001$ (versus control; ANOVA followed by Tukey test). Scale bars: 10 μm.

differential targeting, and we are testing this possibility. The FGF22- and FGF7-containing vesicle each would have its own ‘tag’ on its surface to be recognized by the appropriate adaptor protein. In the case of the neurotrophic factor BDNF, the protein is stored in a vesicle containing a membrane protein, synaptotagmin-IV (Dean et al., 2009). Synaptotagmin-IV regulates BDNF secretion from the vesicles, and it appears to contribute to the specific targeting of BDNF-harboring vesicles (Dean et al., 2009; Dean et al., 2012). Similar membrane molecules might function as ‘tags’ for FGF22- and FGF7-containing vesicles.

An additional interesting finding from our study is that the extent of localization of FGF7 to inhibitory synapses was decreased in

Journal of Cell Science (2015) 128, 281–292 doi:10.1242/jcs.158337

SAP102- and PSD95-knockdown neurons (Fig. 5D). Our live-imaging experiments suggest that SAP102 and PSD95 are not the adaptors for FGF7 transport (Fig. 3B,D,F), and indeed, in SAP102- and PSD95-knockdown neurons, we still found a punctate pattern of FGF7 in the dendrite (Fig. 5A,B). Thus, SAP102 and PSD95 appear to indirectly affect the targeting of FGF7 to inhibitory synapses or its retention at the synapses. In addition, in neurons in which KIF3A or KIF17 function was disrupted, the size of FGF7 puncta or localization of FGF7 to inhibitory synapses was also decreased (Fig. 2C,D). What is common regarding the function of SAP102, PSD95, KIF3A and KIF17 is that they are all involved in the development of excitatory synapses; SAP102 and PSD95 are scaffolding proteins at excitatory synapses and are crucial for their differentiation (Ehrlich et al., 2007; Elias et al., 2008; Elias and Nicoll, 2007; Murata and Constantine-Paton, 2013; Zheng et al., 2011), and KIF3A and KIF17 are involved in AMPA and NMDA receptor transportation (Jo et al., 1999; Lin et al., 2012; Setou et al., 2000). We also found that SAP102 is an adaptor for the targeting of FGF22 to excitatory synapses (Fig. 3A,C,E; Fig. 4) and that KIF3A and KIF17 are involved in the excitatory synaptic targeting of FGF22 (Fig. 1D). Therefore, it is reasonable to speculate that the change in FGF7 localization in SAP102-, PSD95-, KIF3A- or KIF17-inactivated neurons is the consequence of changes in excitatory synaptic differentiation to control the balance between excitatory and inhibitory synapses. In fact, FGF7-dependent inhibitory synapse formation begins after excitatory synapses start to form during development (Terauchi et al., 2010). Our results suggest the interesting possibility that excitatory synapses, once formed, might send signals to promote the targeting of FGF7 to nascent inhibitory synapses to regulate inhibitory synapse formation.

## MATERIALS AND METHODS

### Primary neuronal cultures and transfection

Dissociated hippocampal cultures were prepared from postnatal day (P)0–P1 mice (C57/BL6) as described previously (Terauchi et al., 2010). All animal care and use was in accordance with the institutional guidelines and approved by the Institutional Animal Care and Use Committees at Boston Children's Hospital and University of Michigan. Neurons ($0.35–0.55\times10^5$) were plated on poly-D-lysine-coated glass coverslips (12 mm diameter) or glass-bottomed dishes with a 14-mm glass coverslip (MatTek Corporation), and maintained in neurobasal medium with B27 supplement (Invitrogen). Neurons were transfected by using the calcium phosphate method (CalPhos Mammalian Transfection Kit, Clontech) at 1–7 days *in vitro* (DIV) with 1–4 µg of plasmids per coverslip for 1 h. The transfected cells were analyzed at 5–8 DIV.

### DNA constructs

Expression plasmids for FGF22–GFP and FGF7–GFP were generated by subcloning the full-length mouse *Fgf22* and *Fgf7* cDNA (minus the stop codon) into the *Xho*I–*Sac*II or *Nhe*I–*Xho*I sites of pEGFP-N1 (Clontech) in frame, respectively. Expression plasmids for FGF7–RFP and FGF22–RFP were generated by ligating the full-length mouse *Fgf* cDNA (minus the stop codon) with the *DsRed2* or *mCherry* cDNA (Clontech) in frame and then subcloning the resultant *Fgf–RFP* cDNA into the *Xho*I–*Not*I or *Nhe*I–*Not*I sites of pEGFP-N1 (Clontech). Expression plasmids for GFP–gephyrin and GFP–SAP102 were generated by subcloning the full-length mouse *gephyrin* (amplified by RT-PCR from mouse brain) or *SAP102* cDNA (from Open Biosystems) in frame into the *Xho*I–*Sac*II sites of pEGFP-C2 (Clontech). Expression plasmids for RFP–gephyrin and RFP–SAP102 were generated by ligating the *mCherry* cDNA with the *gephyrin* or *SAP102* cDNA in frame and then subcloning the ligated cDNA into the *Xho*I–*Not*I sites of pEGFP-C2. The expression plasmid for PSD95–GFP was generated by subcloning the full-length rat *PSD95* cDNA (a gift from John Woodward, Medical University of South Carolina) into the *Eco*RI–*Kpn*I sites of pEGFP-N1 in frame. Gephyrin, PSD95 and SAP102 shRNA knockdown plasmids were created by inserting the corresponding oligonucleotides into the HuSH shRNA vector (pRFP-C-RS, OriGene). The following sequences encoding the shRNA were used: gephyrin, 5′-GCCAGCTCTACCTCATGCCATT-GACCTTT-3′; PSD95, 5′-GCCTTCGACAGGGCCACGAAGCTGGA-GCA-3′; and SAP102, 5′-CAAGTCCATTGAAGCACTTATGGAA-ATG-3′. Knockdown efficiency was examined by transfecting shgephyrin and GFP–gephyrin, shPSD95 and PSD95–GFP, or shSAP102 and GFP–SAP102 plasmids into cultured hippocampal neurons and quantifying the reduction of total GFP fluorescence relative to that in control shRNA-transfected neurons (Fig. 4A).

Dominant negative (DN) forms of KIF5, KIF3A and KIF17 were designed to lack the motor domain but still bind to their cargos. The expression plasmid for KIF5DN was as described previously (Falley et al., 2009). Expression plasmids for KIF3ADN and KIF17DN were generated by subcloning a mutant form of human *KIF3A* or human *KIF17* cDNA into the *Eco*RI–*Sal*I sites of pAcGFP-C1 (KIF3ADN) or pAcGFP-C2 (KIF17DN) (Clontech). Primers used for generating the mutant form of KIF3ADN were 5′-CGTGCTAAGAATTCTAAAAAT-3′ and 5′-GTACCGTCGACTTACTGCAG-3′, and those of KIF17DN were 5′-CCAAGGAATTCAGGAACAAGCC-3′ and 5′-GGGTCGACT-AGTTCTAGAGC-3′. KIF3A forms heterodimers with KIF3B (Yamazaki et al., 1995) and KIF5s do so within their family (Hirokawa and Noda, 2008). However, because KIFs restrict their dimerization to within their individual class, they are unlikely to cross-react with each other.

The KIF21B-knockdown plasmid was constructed with pSuper-neo-GFP (OligoEngine) with the following sequence encoding the shRNA: 5′-CCACGATGACTTCAAGTTC-3′. The scrambled sequence for control shRNA was: 5′-GCGCGCTTTGTAGGATTCG-3′. The knockdown efficiency was verified by a massive reduction in the amount of KIF21B as shown by immunostaining and western blotting (Labonté et al., 2013).

### Immunocytochemistry

Cultured neurons were fixed with 3% paraformaldehyde (PFA) for 10 min at 37℃ and blocked in 2% BSA, 2% normal goat serum and 0.1% Triton X-100 for 1 h, followed by incubation with primary antibodies overnight at 4℃. Secondary antibodies were applied for 1 h at room temperature, and samples were mounted with p-phenylenediamine. Dilutions and sources of antibodies used are as follows: chicken anti-GFP (1:500, Millipore; or 1:2500, Aves Labs), mouse anti-GFP (clone 3E6, 1:100, Millipore), rabbit anti-DsRed and mouse anti-DsRed (1:500 and 1:600, Clontech), anti-PSD95 (clone K28/43, 1:250, NeuroMab), anti-gephyrin (clone mAb7a, 1:150, Synaptic Systems), anti-VGAT (1:1500, Synaptic Systems) and anti-VGLUT1 (1:5000, Millipore).

### Imaging

An epifluorescent microscope (Olympus, BX61) was used to acquire 12-bit images with 20× and 40× objectives and F-View II CCD camera (Soft Imaging System) at a resolution of 1376×1032 pixels. Alternatively, images were acquired on confocal microscopes (Olympus, FV1000 and Zeiss LSM 700) using 40× and 60× objectives with 1.0× or 1.5× zoom at a resolution of 1024×1024 pixels. For each experiment, all images were acquired with identical settings for the laser power, detector gain and amplifier offset. Confocal images were acquired as a *z*-stack (10–15 optical sections, 0.5-µm step size). For quantification, neurites or fields (222.85×167.86 µm for pictures taken with Olympus BX61, 317.13×158.5 µm for pictures taken with Olympus FV1000 and 159.89×159.89 µm for pictures taken with Zeiss LSM 700) were randomly selected and thresholded (the intensity of the dendritic shaft in control cultures was calculated as the background fluorescence), and the average size, density (per length) and average intensity of puncta were quantified with MetaMorph Software. MetaMorph Software was also used for determining the colocalization indices. Images of single fluorescence channels were thresholded and binarized, and an object was considered to colocalize with another object if its area overlapped with the signal in the second channel.

### Live imaging

Imaging was conducted on a Nikon Eclipse Ti microscope using a 60× Nikon Plan Apo VC oil objective lens at a resolution of 1392×1040 pixels. Fluorophores were excited using a Lambda XL lamp (Sutter Instrument) together with detection filters specific for GFP (GFP-L HYQ, Nikon) and mCherry (TX RED HYQ, Nikon). During the imaging, MatTek dishes were incubated in a stage top incubator (TOKAI HIT). Images (149.63×111.80 µm) were collected every 5 s, with each scan time no longer than 800 ms. For dual-color imaging, each color image was collected sequentially to avoid bleed-through. Images were acquired with a CoolSNAP HQ CCD camera (Photometrics), and quantified using NIS-Elements Software (Nikon). For the analysis, puncta in dendrites were observed for 45 s. Puncta moving for the entire 45 s were defined as moving puncta. For the quantification of puncta colocalization, an object was considered to colocalize with another object if >25% of its area was covered by the signal in the second channel. Two puncta were considered to be moving together if they were traveling along the dendrite together for 45 s. For the velocity analysis, a detection filter for mCherry was used to detect FGF7–RFP and FGF22–RFP puncta. The total distances that they moved in 45 s were quantified, and the distance per second was calculated as their velocity.

### Acknowledgements

We thank M. Zhang and P. Yee for technical assistance and E. Piell for help with plasmid construction.

### Competing interests

The authors declare no competing or financial interests.

### Author contributions

H.U. and A.T. designed experiments and prepared the manuscript. A.T., K.M.T. and K.K. performed experiments. Y.P. and M.K. provided unpublished materials. H.U. supervised the project.

### Funding

This work was supported by the National Institutes of Health [grant number NS070005 to H.U.]; and Deutsche Forschungsgemeinschaft [grant numbers DFG KN556/6-1 and GRK1459 to M.K.]. Deposited in PMC for release after 12 months.

### Supplementary material

Supplementary material available online at
http://jcs.biologists.org/lookup/suppl/doi:10.1242/jcs.158337/-/DC1

### References

**Adachi, N., Kohara, K. and Tsumoto, T.** (2005). Difference in trafficking of brain-derived neurotrophic factor between axons and dendrites of cortical neurons, revealed by live-cell imaging. *BMC Neurosci.* **6**, 42.

**Bellone, C. and Nicoll, R. A.** (2007). Rapid bidirectional switching of synaptic NMDA receptors. *Neuron* **55**, 779-785.

**Chen, B. S., Gray, J. A., Sanz-Clemente, A., Wei, Z., Thomas, E. V., Nicoll, R. A. and Roche, K. W.** (2012). SAP102 mediates synaptic clearance of NMDA receptors. *Cell Reports* **2**, 1120-1128.

**Chu, P. J., Rivera, J. F. and Arnold, D. B.** (2006). A role for Kif17 in transport of Kv4.2. *J. Biol. Chem.* **281**, 365-373.

**Dalva, M. B., McClelland, A. C. and Kayser, M. S.** (2007). Cell adhesion molecules: signalling functions at the synapse. *Nat. Rev. Neurosci.* **8**, 206-220.

**Dean, C., Liu, H., Dunning, F. M., Chang, P. Y., Jackson, M. B. and Chapman, E. R.** (2009). Synaptotagmin-IV modulates synaptic function and long-term potentiation by regulating BDNF release. *Nat. Neurosci.* **12**, 767-776.

**Dean, C., Liu, H., Staudt, T., Stahlberg, M. A., Vingill, S., Bückers, J., Kamin, D., Engelhardt, J., Jackson, M. B., Hell, S. W. et al.** (2012). Distinct subsets of Syt-IV/BDNF vesicles are sorted to axons versus dendrites and recruited to synapses by activity. *J. Neurosci.* **32**, 5398-5413.

**Dumoulin, A., Triller, A. and Kneussel, M.** (2009). Cellular transport and membrane dynamics of the glycine receptor. *Front. Mol. Neurosci.* **2**, 28.

**Ehrlich, I., Klein, M., Rumpel, S. and Malinow, R.** (2007). PSD-95 is required for activity-driven synapse stabilization. *Proc. Natl. Acad. Sci. USA* **104**, 4176-4181.

**Elias, G. M. and Nicoll, R. A.** (2007). Synaptic trafficking of glutamate receptors by MAGUK scaffolding proteins. *Trends Cell Biol.* **17**, 343-352.

**Elias, G. M., Elias, L. A., Apostolides, P. F., Kriegstein, A. R. and Nicoll, R. A.** (2008). Differential trafficking of AMPA and NMDA receptors by SAP102 and PSD-95 underlies synapse development. *Proc. Natl. Acad. Sci. USA* **105**, 20953-20958.

**Falley, K., Schütt, J., Iglauer, P., Menke, K., Maas, C., Kneussel, M., Kindler, S., Wouters, F. S., Richter, D. and Kreienkamp, H. J.** (2009). Shank1 mRNA: dendritic transport by kinesin and translational control by the 5'untranslated region. *Traffic* **10**, 844-857.

**Fox, M. A. and Umemori, H.** (2006). Seeking long-term relationship: axon and target communicate to organize synaptic differentiation. *J. Neurochem.* **97**, 1215-1231.

**Fox, M. A., Sanes, J. R., Borza, D. B., Eswarakumar, V. P., Fässler, R., Hudson, B. G., John, S. W., Ninomiya, Y., Pedchenko, V., Pfaff, S. L. et al.** (2007). Distinct target-derived signals organize formation, maturation, and maintenance of motor nerve terminals. *Cell* **129**, 179-193.

**Futai, K., Doty, C. D., Baek, B., Ryu, J. and Sheng, M.** (2013). Specific trans-synaptic interaction with inhibitory interneuronal neurexin underlies differential ability of neuroligins to induce functional inhibitory synapses. *J. Neurosci.* **33**, 3612-3623.

**Guillaud, L., Setou, M. and Hirokawa, N.** (2003). KIF17 dynamics and regulation of NR2B trafficking in hippocampal neurons. *J. Neurosci.* **23**, 131-140.

**Hirokawa, N. and Noda, Y.** (2008). Intracellular transport and kinesin superfamily proteins, KIFs: structure, function, and dynamics. *Physiol. Rev.* **88**, 1089-1118.

**Hirokawa, N., Noda, Y., Tanaka, Y. and Niwa, S.** (2009). Kinesin superfamily motor proteins and intracellular transport. *Nat. Rev. Mol. Cell Biol.* **10**, 682-696.

**Hirokawa, N., Niwa, S. and Tanaka, Y.** (2010). Molecular motors in neurons: transport mechanisms and roles in brain function, development, and disease. *Neuron* **68**, 610-638.

**Jeyifous, O., Waites, C. L., Specht, C. G., Fujisawa, S., Schubert, M., Lin, E. I., Marshall, J., Aoki, C., de Silva, T., Montgomery, J. M. et al.** (2009). SAP97 and CASK mediate sorting of NMDA receptors through a previously unknown secretory pathway. *Nat. Neurosci.* **12**, 1011-1019.

**Jo, K., Derin, R., Li, M. and Bredt, D. S.** (1999). Characterization of MALS/Velis-1, -2, and -3: a family of mammalian LIN-7 homologs enriched at brain synapses in association with the postsynaptic density-95/NMDA receptor postsynaptic complex. *J. Neurosci.* **19**, 4189-4199.

**Johnson-Venkatesh, E. M. and Umemori, H.** (2010). Secreted factors as synaptic organizers. *Eur. J. Neurosci.* **32**, 181-190.

**Kardon, J. R. and Vale, R. D.** (2009). Regulators of the cytoplasmic dynein motor. *Nat. Rev. Mol. Cell Biol.* **10**, 854-865.

**Kneussel, M.** (2005). Postsynaptic scaffold proteins at non-synaptic sites. The role of postsynaptic scaffold proteins in motor-protein-receptor complexes. *EMBO Rep.* **6**, 22-27.

**Kneussel, M. and Wagner, W.** (2013). Myosin motors at neuronal synapses: drivers of membrane transport and actin dynamics. *Nat. Rev. Neurosci.* **14**, 233-247.

**Labonté, D., Thies, E., Pechmann, Y., Groffen, A. J., Verhage, M., Smit, A. B., van Kesteren, R. E. and Kneussel, M.** (2013). TRIM3 regulates the motility of the kinesin motor protein KIF21B. *PLoS ONE* **8**, e75603.

**Lau, C. G. and Zukin, R. S.** (2007). NMDA receptor trafficking in synaptic plasticity and neuropsychiatric disorders. *Nat. Rev. Neurosci.* **8**, 413-426.

**Lin, Y., Jones, B. W., Liu, A., Vazquéz-Chona, F. R., Lauritzen, J. S., Ferrell, W. D. and Marc, R. E.** (2012). Rapid glutamate receptor 2 trafficking during retinal degeneration. *Mol. Neurodegener.* **7**, 7.

**Linhoff, M. W., Laurén, J., Cassidy, R. M., Dobie, F. A., Takahashi, H., Nygaard, H. B., Airaksinen, M. S., Strittmatter, S. M. and Craig, A. M.** (2009). An unbiased expression screen for synaptogenic proteins identifies the LRRTM protein family as synaptic organizers. *Neuron* **61**, 734-749.

**Maas, C., Tagnaouti, N., Loebrich, S., Behrend, B., Lappe-Siefke, C. and Kneussel, M.** (2006). Neuronal cotransport of glycine receptor and the scaffold protein gephyrin. *J. Cell Biol.* **172**, 441-451.

**Maas, C., Belgardt, D., Lee, H. K., Heisler, F. F., Lappe-Siefke, C., Magiera, M. M., van Dijk, J., Hausrat, T. J., Janke, C. and Kneussel, M.** (2009). Synaptic activation modifies microtubules underlying transport of postsynaptic cargo. *Proc. Natl. Acad. Sci. USA* **106**, 8731-8736.

**Mandal, M., Wei, J., Zhong, P., Cheng, J., Duffney, L. J., Liu, W., Yuen, E. Y., Twelvetrees, A. E., Li, S., Li, X. J. et al.** (2011). Impaired alpha-amino-3-hydroxy-5-methyl-4-isoxazolepropionic acid (AMPA) receptor trafficking and function by mutant huntingtin. *J. Biol. Chem.* **286**, 33719-33728.

**Marszalek, J. R., Weiner, J. A., Farlow, S. J., Chun, J. and Goldstein, L. S.** (1999). Novel dendritic kinesin sorting identified by different process targeting of two related kinesins: KIF21A and KIF21B. *J. Cell Biol.* **145**, 469-479.

**Millecamps, S. and Julien, J. P.** (2013). Axonal transport deficits and neurodegenerative diseases. *Nat. Rev. Neurosci.* **14**, 161-176.

**Missler, M., Südhof, T. C. and Biederer, T.** (2012). Synaptic cell adhesion. *Cold Spring Harb. Perspect. Biol.* **4**, a005694.

**Möhler, H.** (2006). GABAA receptors in central nervous system disease: anxiety, epilepsy, and insomnia. *J. Recept. Signal Transduct. Res.* **26**, 731-740.

**Murata, Y. and Constantine-Paton, M.** (2013). Postsynaptic density scaffold SAP102 regulates cortical synapse development through EphB and PAK signaling pathway. *J. Neurosci.* **33**, 5040-5052.

**Nakajima, K., Yin, X., Takei, Y., Seog, D. H., Homma, N. and Hirokawa, N.** (2012). Molecular motor KIF5A is essential for GABA(A) receptor transport, and KIF5A deletion causes epilepsy. *Neuron* **76**, 945-961.

**Rubenstein, J. L. and Merzenich, M. M.** (2003). Model of autism: increased ratio of excitation/inhibition in key neural systems. *Genes Brain Behav.* **2**, 255-267.

**Sans, N., Petralia, R. S., Wang, Y. X., Blahos, J., 2nd, Hell, J. W. and Wenthold, R. J.** (2000). A developmental change in NMDA receptor-associated proteins at hippocampal synapses. *J. Neurosci.* **20**, 1260-1271.

**Sans, N., Prybylowski, K., Petralia, R. S., Chang, K., Wang, Y. X., Racca, C., Vicini, S. and Wenthold, R. J.** (2003). NMDA receptor trafficking through an interaction between PDZ proteins and the exocyst complex. *Nat. Cell Biol.* **5**, 520-530.
**Sanz-Clemente, A., Nicoll, R. A. and Roche, K. W.** (2013). Diversity in NMDA receptor composition: many regulators, many consequences. *Neuroscientist* **19**, 62-75.
**Sathish, N., Zhu, F. X. and Yuan, Y.** (2009). Kaposi's sarcoma-associated herpesvirus ORF45 interacts with kinesin-2 transporting viral capsid-tegument complexes along microtubules. *PLoS Pathog.* **5**, e1000332.
**Setou, M., Nakagawa, T., Seog, D. H. and Hirokawa, N.** (2000). Kinesin superfamily motor protein KIF17 and mLin-10 in NMDA receptor-containing vesicle transport. *Science* **288**, 1796-1802.
**Setou, M., Seog, D. H., Tanaka, Y., Kanai, Y., Takei, Y., Kawagishi, M. and Hirokawa, N.** (2002). Glutamate-receptor-interacting protein GRIP1 directly steers kinesin to dendrites. *Nature* **417**, 83-87.
**Siddiqui, T. J. and Craig, A. M.** (2011). Synaptic organizing complexes. *Curr. Opin. Neurobiol.* **21**, 132-143.
**Singer, H. S. and Minzer, K.** (2003). Neurobiology of Tourette's syndrome: concepts of neuroanatomic localization and neurochemical abnormalities. *Brain Dev.* **25 Suppl. 1**, S70-S84.
**Smith, M. J., Pozo, K., Brickley, K. and Stephenson, F. A.** (2006). Mapping the GRIF-1 binding domain of the kinesin, KIF5C, substantiates a role for GRIF-1 as an adaptor protein in the anterograde trafficking of cargoes. *J. Biol. Chem.* **281**, 27216-27228.
**Südhof, T. C.** (2008). Neuroligins and neurexins link synaptic function to cognitive disease. *Nature* **455**, 903-911.
**Terauchi, A. and Umemori, H.** (2012). Specific sets of intrinsic and extrinsic factors drive excitatory and inhibitory circuit formation. *Neuroscientist* **18**, 271-286.
**Terauchi, A., Johnson-Venkatesh, E. M., Toth, A. B., Javed, D., Sutton, M. A. and Umemori, H.** (2010). Distinct FGFs promote differentiation of excitatory and inhibitory synapses. *Nature* **465**, 783-787.
**Toth, A. B., Terauchi, A., Zhang, L. Y., Johnson-Venkatesh, E. M., Larsen, D. J., Sutton, M. A. and Umemori, H.** (2013). Synapse maturation by activity-dependent ectodomain shedding of SIRPα. *Nat. Neurosci.* **16**, 1417-1425.
**Twelvetrees, A. E., Yuen, E. Y., Arancibia-Carcamo, I. L., MacAskill, A. F., Rostaing, P., Lumb, M. J., Humbert, S., Triller, A., Saudou, F., Yan, Z. et al.** (2010). Delivery of GABAARs to synapses is mediated by HAP1-KIF5 and disrupted by mutant huntingtin. *Neuron* **65**, 53-65.
**Tyagarajan, S. K. and Fritschy, J. M.** (2014). Gephyrin: a master regulator of neuronal function? *Nat. Rev. Neurosci.* **15**, 141-156.
**Uchida, A., Alami, N. H. and Brown, A.** (2009). Tight functional coupling of kinesin-1A and dynein motors in the bidirectional transport of neurofilaments. *Mol. Biol. Cell* **20**, 4997-5006.
**Umemori, H. and Sanes, J. R.** (2008). Signal regulatory proteins (SIRPS) are secreted presynaptic organizing molecules. *J. Biol. Chem.* **283**, 34053-34061.
**Umemori, H., Linhoff, M. W., Ornitz, D. M. and Sanes, J. R.** (2004). FGF22 and its close relatives are presynaptic organizing molecules in the mammalian brain. *Cell* **118**, 257-270.
**Waites, C. L., Craig, A. M. and Garner, C. C.** (2005). Mechanisms of vertebrate synaptogenesis. *Annu. Rev. Neurosci.* **28**, 251-274.
**Washbourne, P., Liu, X. B., Jones, E. G. and McAllister, A. K.** (2004). Cycling of NMDA receptors during trafficking in neurons before synapse formation. *J. Neurosci.* **24**, 8253-8264.
**Wassef, A., Baker, J. and Kochan, L. D.** (2003). GABA and schizophrenia: a review of basic science and clinical studies. *J. Clin. Psychopharmacol.* **23**, 601-640.
**Yamazaki, H., Nakata, T., Okada, Y. and Hirokawa, N.** (1995). KIF3A/B: a heterodimeric kinesin superfamily protein that works as a microtubule plus end-directed motor for membrane organelle transport. *J. Cell Biol.* **130**, 1387-1399.
**Zheng, C. Y., Seabold, G. K., Horak, M. and Petralia, R. S.** (2011). MAGUKs, synaptic development, and synaptic plasticity. *Neuroscientist* **17**, 493-512.